1 # Routine monitoring of Western Lake Erie to track water quality

2 # changes associated with cyanobacterial harmful algal blooms

3

4 Anna G Boegehold[1],  Ashley M. Burtner[1], Andrew C Camilleri[1], Glenn Carter[1], Paul DenUyl[1],
5 David Fanslow[2], Deanna Fyffe Semenyuk[1,3], Casey M Godwin[1], Duane Gossiaux[2], Thomas H
6 Johengen[1], Holly Kelchner[1], Christine Kitchens[1], Lacey A. Mason[2], Kelly McCabe[1], Danna
7 Palladino[2], Dack Stuart[1,4], Henry Vanderploeg[2], Reagan Errera[2]
8
9
10 [1]Cooperative Institute for Great Lakes Research (CIGLR), University of Michigan, 4840 South
11 State Road, Ann Arbor, MI 48108, USA
12 [2]NOAA Great Lakes Environmental Research Laboratory, 4840 South State Road, Ann Arbor,
13 MI 48108, USA
14 [3]Jacobs, 1999 Bryan Street, Suite 1200, Dallas, TX, 75201, USA
15 [4]Woods Hole Group, Inc., 107 Waterhouse Road, Bourne, MA 02532
16
17 *Correspondence to:* Anna G Boegehold (annaboeg@umich.edu) & Reagan Errera
18 (reagan.errera@noaa.gov)

# Abstract

The western basin of Lake Erie has a history of recurrent cyanobacterial harmful algal blooms (HABs) despite decades of efforts by the United States and Canada to limit phosphorus loading, a major driver of the blooms. In response, the National Oceanic and Atmospheric Administration (NOAA) Great Lakes Environmental Research Laboratory (GLERL) and the Cooperative Institute for Great Lakes Research (CIGLR) created an annual sampling program to detect, monitor, assess, and predict HABs in western Lake Erie. Here we describe the data collected from this monitoring program from 2012 to 2021. This dataset includes observations on physico-chemical properties, major nutrient fractions, phytoplankton pigments, microcystins, and optical properties for western Lake Erie. This dataset is particularly relevant for creating models, verifying and calibrating remote sensing algorithms, and informing experimental research to further understand the water quality dynamics that influence HABs in this internationally significant body of freshwater. The dataset can be freely accessed from NOAA National Centers for Environmental Information (NCEI) at https://doi.org/10.25921/11da-3x54 (Cooperative Institute for Great Lakes Research, University of Michigan; NOAA Great Lakes Environmental Research Laboratory, 2019).

# Introduction

35

36         Lake Erie is situated on the international boundary between the United States and

37    Canada and is the smallest by volume of the five Laurentian Great Lakes. It is ecologically,

38    culturally, and economically significant to the approximately 12.5 million people who live in the

39    watershed. Each year Lake Erie supports nearly 14,000 tonnes of commercial and traditional

40    fisheries, over 33,000,000 tonnes of freight, and over $1.5 million in recreation and tourism

41    business (Sterner et al., 2020). Lake Erie has endured multiple anthropogenic stressors since

42    European settlement in the area, most notably the draining of coastal wetlands for development

43    of agricultural lands in the late 18th century (Allinger and Reavie, 2013). Currently, the

44    ecological state of Lake Erie is considered poor, partially due to excess nutrient input that

45    supports harmful algal blooms (HABs; ECCC and US EPA, 2022). These seasonal HABs are

46    typically dominated by toxin producing cyanobacteria, causing concern for public and

47    ecosystem health (Watson et al., 2016). Humans can be exposed to cyanotoxins through

48    ingestion of contaminated fish and drinking water and through inhalation and dermal exposure

49    during recreational events such as swimming and boating (Carmichael and Boyer, 2016; Buratti

50    et al., 2017). Cyanotoxins can also cause illness and death in aquatic and terrestrial animals

51    (Carmichael and Boyer, 2016). The economic cost of HABs impacts in Lake Erie is estimated to

52    be hundreds of millions of dollars each year (Smith et al., 2019).

53         To combat the deteriorated state of Lake Erie water quality, bi-national water resource

54    management policies alongside scientific research and water quality monitoring efforts have

55    been underway for decades. The Great Lakes Water Quality Agreement (GLWQA), first signed

56    in 1972, was a commitment between the US and Canada in response to degraded water quality

57    throughout the Great Lakes ecosystem (GLWQA, 2012). Phosphorus was found to be the key

58    nutrient that was promoting excess phytoplankton growth (Charlton et al., 1993), and thus the

59    GLWQA sought to limit total phosphorus input to the lakes in an attempt to reduce

60  phytoplankton growth and biomass (Steffen et al., 2014). The 1972 Clean Water Act (CWA) was

61  similarly enacted to regulate point-source pollution discharge, including phosphorus, into

62  navigable waters in the United States. After the signing and implementation of the phosphorus

63  load reduction practices outlined in the GLWQA and CWA, the water quality of Lake Erie

64  improved and the lake experienced a period of restoration (Makarewicz and Bertram, 1991).

65  This success was attributed to upgrades to sewage treatment plants and industrial discharges

66  which reduced phosphorus loading from point sources by 50% within ten years of peak levels

67  observed in 1968 (Charlton et al., 1993; Joosse and Baker, 2011; Steffen et al., 2014).

68       While the water quality of Lake Erie rebounded in the 1980s and early 1990s, by the mid

69  1990s and early 2000s annual HAB events were occurring in Lake Erie again, particularly in the

70  warm, shallow western basin (Allinger and Reavie, 2013; Kane et al., 2015; Watson et al.,

71  2016). Total phosphorus loading has been relatively stable in Lake Erie from the 1980s onward

72  (Dolan and Chapra, 2012; Watson et al., 2016), and although point-source phosphorus loading

73  controls had been a successful mitigation measure at one point, several anthropogenic

74  stressors within the watershed were exacerbating the issue of poor water quality. An increase in

75  agricultural sources of biologically available soluble nutrients, legacy phosphorus in the Lake

76  Erie watershed, altered nutrient cycling by invasive dreissenid mussels, and climate change are

77  thought to be primarily responsible for the HABs resurgence (Vanderploeg et al., 2001; Conroy

78  et al., 2005; Bridoux et al., 2010; Michalak et al., 2013; Matisoff et al., 2016; Huisman et al.,

79  2018; Van Meter et al., 2021).

80       The post-recovery period HABs have predominantly been composed of the

81  cyanobacteria species *Microcystis aeruginosa* along with genera *Anabaena, Aphanizomenon,*

82  *Dolichospermum,* and *Planktothrix* (Steffen et al., 2014; Watson et al., 2016). These

83  cyanobacteria can produce an array of several types of phycotoxins, with the most common

84  being a suite of hepatotoxins known as microcystins (MCs). Microcystins primarily affect the

85  liver but can also cause adverse health effects on the kidneys, brain, and reproductive organs

86    (Carmichael and Boyer, 2016). Phycotoxins are commonly present during Lake Erie HABs, and

87    in August 2014 the city of Toledo, OH drinking water supply was contaminated with MCs,

88    leaving >400,000 without clean drinking water (Steffen et al., 2017).

89        To understand HAB events in US waterways, Congress authorized the Harmful Algal

90    Bloom and Hypoxia Research and Control Act in 1998 (HABHRCA; Public Law 115-423) which

91    mandated the National Oceanic and Atmospheric Administration (NOAA) to "advance the

92    scientific understanding and ability to detect, monitor, assess, and predict HAB and hypoxia

93    events". Under HABHRCA, the NOAA Great Lakes Environmental Research Lab (GLERL),

94    NOAA National Centers for Coastal Ocean Science (NCCOS), and the Cooperative Institute for

95    Great Lakes Research (CIGLR; formerly CILER - Cooperative Institute for Limnology and

96    Ecosystems Research) developed an ecological forecast to predict HAB events in Lake Erie.

97    Starting in 2008, researchers at these institutes began using remote sensing to monitor

98    seasonal HABs, created a seasonal forecast system based on spring P loads, and developed

99    models to predict short-term bloom changes to alert stakeholders and the public (Rowe et al.,

100   2016). Products from these efforts, known as Lake Erie Harmful Algal Bloom Forecasts, are

101   freely available during the bloom season at https://coastalscience.noaa.gov/research/stressor-

102   impacts-mitigation/hab-forecasts/lake-erie/.

103       *In-situ* sampling of the bloom was necessary to calibrate and validate the remote

104   sensing images and models as well as measure microcystin concentration. Sampling events

105   were led by personnel at GLERL and CIGLR starting in 2008 and were designed to collect

106   discrete samples within the extent of the bloom area. At first, samples were taken

107   opportunistically within the bloom and sampling locations and analytical parameters were

108   inconsistent. In 2009, regular sampling stations were identified based on spatial patterns of the

109   bloom. From 2009 to 2011, in addition to opportunistic samples, nine main stations in the

110   western basin of Lake Erie were sampled intermittently from June through October (Bertani et

111   al., 2017; Rowland et al., 2020). While these sampling efforts initially began to complement

112    existing research products, the experimental nature of the 2008 to 2011 sampling cruises also

113    provided insight into creating a regular monitoring program that would support critical research

114    and product development related to western Lake Erie HABs.

115         In 2012, researchers at GLERL and CIGLR, with support from the Great Lakes

116    Restoration Initiative (GLRI), formalized a sampling regimen to monitor the spatial and temporal

117    variability of seasonal HAB events in western Lake Erie (WLE). The establishment of this

118    monitoring program corresponded with increased federal emphasis on evaluating trends and

119    drivers of WLE HABs and water quality. Four monitoring stations were identified and regular

120    surface samples were collected from May to September and analyzed for nutrient, pigment, and

121    particulate microcystin concentrations (Figs. 1 & 2). In following years, the monitoring program

122    evolved and expanded. New stations were added to better characterize the bloom and

123    complement other observing systems. Sampling parameters were adjusted and added based on

124    the needs of current research (Table 1). Results of these sampling cruises were compiled and

125    distributed informally upon request until 2019 when the data were organized and archived on

126    the NOAA National Centers for Environmental Information (NCEI) open-access data repository

127    (https://www.ncei.noaa.gov/).

128         Long term monitoring of WLE is fundamental to the continual assessment of water

129    quality changes in response to both stressors and water quality management efforts (Hartig et

130    al., 2009, 2021). The GLERL/CIGLR monitoring data has been used by numerous researchers

131    to develop and assess models (Rowe et al., 2016; Weiskerger et al., 2018; Fang et al., 2019;

132    Liu et al., 2020; Qian et al., 2021; Wang and Boegman, 2021; Hellweger et al., 2022; Maguire et

133    al., 2022), to calibrate remote sensing algorithms (Sayers et al., 2016, 2019; Avouris and Ortiz,

134    2019; Bosse et al., 2019; Vander Woude et al., 2019; Pirasteh et al., 2020; Xu et al., 2022), and

135    to elucidate ecological mechanisms and complement experimental data (Cory et al., 2016;

136    Reavie et al., 2016; Berry et al., 2017; Steffen et al., 2017; Kharbush et al., 2019, 2023; Newell

137    et al., 2019; Den Uyl et al., 2021; Smith et al., 2021, 2022; Hoffman et al., 2022; Marino et al.,

138    2022; Yancey et al., 2022a, b).

139        The objective of this paper is to inform users of the dataset "Physical, chemical, and

140    biological water quality monitoring data to support detection of Harmful Algal Blooms (HABs) in

141    western Lake Erie, collected by the Great Lakes Environmental Research Laboratory and the

142    Cooperative Institute for Great Lakes Research since 2012" by describing the data generated

143    from this monitoring program and detailing how samples were collected and analyzed. This

144    paper contextualizes this long-term data set so that it can continue to be used to benefit our

145    collective ecological knowledge of western Lake Erie.

146

147    Table 1. Description of stations sampled in western Lake Erie from 2012 to 2021. Latitude and

148    longitude (decimal degree) coordinates for each station are target locations as the boat was

149    allowed to drift at each site during *in-situ* sampling.

150

| Station | Latitude | Longitude | Avg. Depth (m) | Years Monitored |
|---------|----------|-----------|----------------|-----------------|
| WE02 | 41.762 | -83.330 | 5.4 | 2012-2021 |
| WE04 | 41.827 | -83.193 | 8.4 | 2012-2021 |
| WE06 | 41.705 | -83.385 | 2.9 | 2012-2021 |
| WE08 | 41.834 | -83.364 | 4.8 | 2012-2021 |
| WE09 | 41.718 | -83.424 | 2.7 | 2016-2021 |
| WE12 | 41.703 | -83.254 | 6.6 | 2014-2021 |
| WE13 | 41.741 | -83.136 | 8.9 | 2014-2021 |
| WE14 | 41.720 | -83.010 | 9.3 | 2015 |
| WE15 | 41.617 | -83.009 | 4.5 | 2015-2017 |
| WE16 | 41.660 | -83.143 | 6.2 | 2018-2021 |

151

# Methods

## Study Site

Based on the lake's bathymetry, Lake Erie can be divided into the eastern, central, and western basins which in turn influence physical and biological processes (Allinger and Reavie, 2013). The data presented in this paper were collected from the western basin, which encompasses the western part of the lake to Point Pelee, ON, Canada and Cedar Point, OH, USA (Fig. 1). The well-mixed western basin is the shallowest (maximum average depth of 11 m), warmest, and most productive of the three basins. Although it's typical for temperate WLE to have ice cover in the winter (Jan to Mar), summer (Jul to Sep) surface water temperatures often reach or exceed 25 °C. The western basin receives 95% of its hydraulic inflow from the Detroit River, which connects Lake Erie hydrologically to Lake Huron via the St. Clair River and Lake St. Clair (Cousino et al., 2015). Among the other tributaries to WLE (including River Raisin, Portage River, Ottawa River, Stony Creek, Swan Creek, and Sandusky River), the Maumee River discharges into the western basin near the city of Toledo, Ohio and contributes a significant amount of sediments and nutrients to the entire Lake Erie basin (Baker et al., 2014a, b; Rowland et al. 2020; see NCWQR 2022 for Maumee River water quality data). Nutrient and sediment loads from the Maumee River can vary with precipitation, where stormwater runoff can provide a pulse of nutrients into the basin, potentially altering cyanobacteria dynamics (Baker et al., 2014a; King et al., 2022). Land use in the Lake Erie watershed is 75% agricultural and 11% urban, both of which contribute to the large amounts of soluble reactive phosphorus into the basin (Mohamed et al., 2019; Myers et al., 2000).

This dataset includes water quality data from ten monitoring stations on the United States side of WLE that were sampled from 2012 to 2021 (Figs. 1 & 2, Tables 1 & 2). The

175 average depth of monitoring stations ranged from 2.7 m at WE9 to 9.3 m at WE14. These sites

176 were chosen to reflect the various nutrient and hydrologic inputs and gradients into WLE, as

177 well as represent areas of the basin that are prone to HABs. The Maumee River inflow was a

178 major consideration in determining these sites. The initial 4 stations sampled in this program

179 (WE02, WE04, WE06, and WE08) were selected because they were consistently within the

180 WLE blooms occurring at the time. Additional sites were later added to better represent the

181 spatial extent of HABs and to augment existing data provided by moored buoy continuous

182 monitoring systems, advanced monitoring technologies, such as Environmental Sample

183 Processors (Den Uyl et al., 2022), and other monitoring programs in WLE.


## 184 Field Sampling

185  Western Lake Erie discrete field sampling was accomplished using NOAA GLERL

186 research vessels. Sampling took place during ice-free months and aimed to quantify the

187 environmental conditions prior to, during, and at the end of the bloom (Fig. 2). Sampling stations

188 represent approximate locations (Table 1; Fig. 1); *in situ* measurements and sampling were

189 collected once the boat reached the targeted location and then proceeded to drift during

190 sampling. The frequency and timing of those cruises varied over the first few years but has been

191 consistent since 2017 (Fig. 2). Sampling was disrupted in 2020 due to the global COVID-19

192 pandemic and resulting public health restrictions. In 2020, sampling was initiated in mid-June at

193 a reduced number of sites for select water quality parameters. In July, sampling stations and

194 parameters were expanded and all stations and parameters were sampled and measured by

195 August 2020. The prior standard sampling schedule resumed in April 2021.
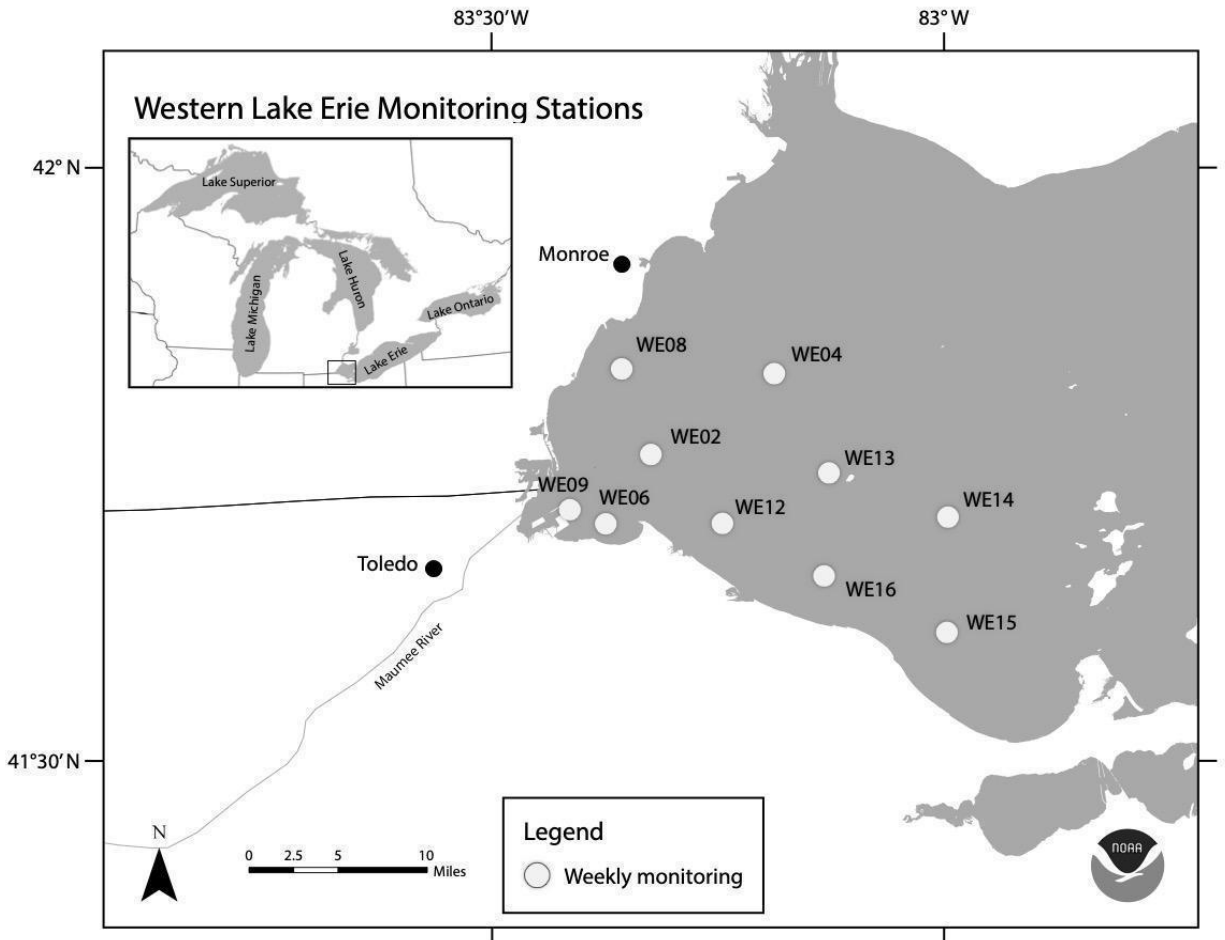
Figure 1. Location of western Lake Erie water quality monitoring stations. This map was provided by NOAA for use in this publication.

199
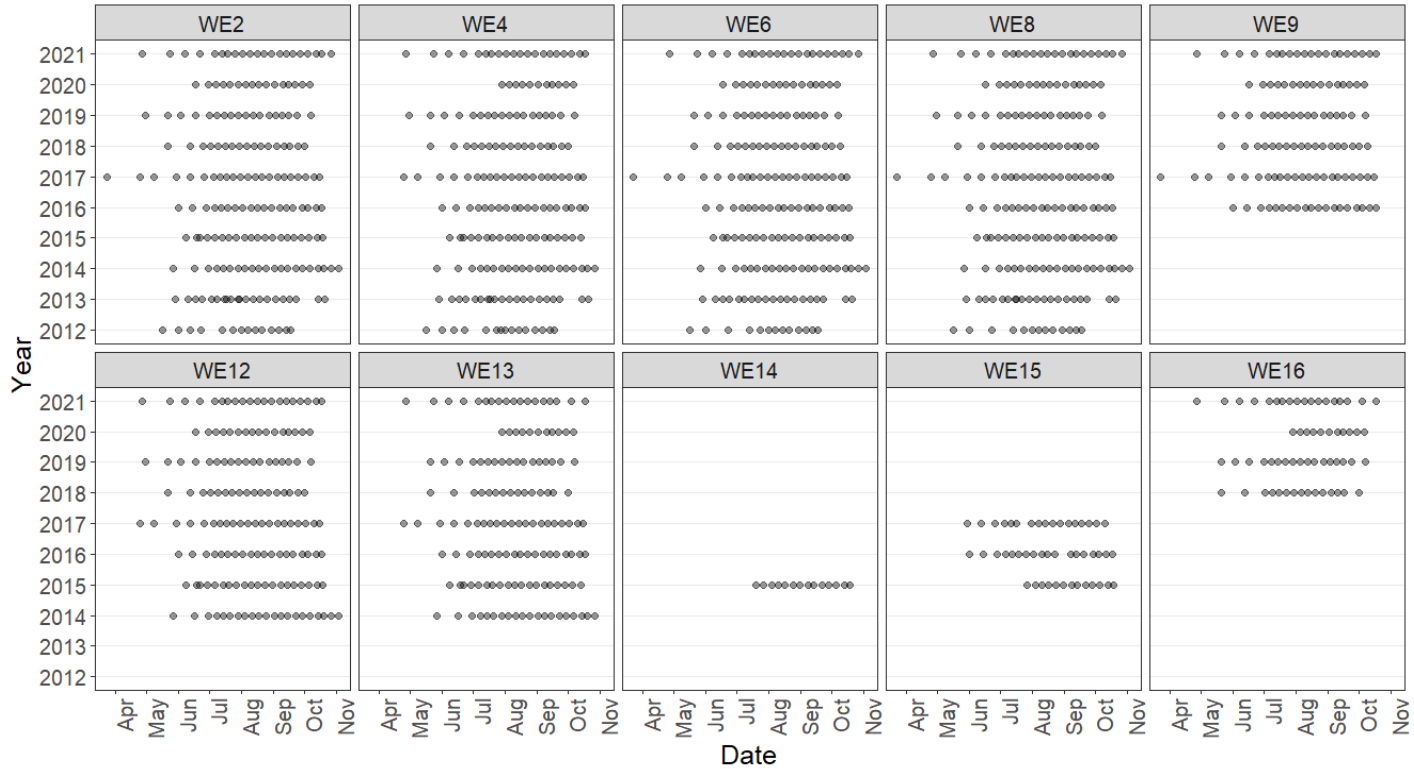
Figure 2. Sampling frequency for each monitoring station for years sampled between 2012 to

201    2021.

202

203    *In-situ* measurements for conductivity, temperature, dissolved oxygen (DO), beam

204    attenuation, transmission, and photosynthetically active radiation (PAR) were taken with a Sea-

205    Bird 19plus V2 conductivity, temperature, and depth (CTD) profiler attached to a hydraulic

206    crane. Data were collected on the downcast and were reported as the mean of recorded values

207    within ± 0.5 m of the discrete sample depth. In 2012, sample temperature was taken on the boat

208    with a Vee Gee Scientific IP67-rated digital thermometer. Sky conditions were recorded at the

209    discretion of the field technician at each station during the sampling cruise. A Secchi disk was

210    lowered into the water on the shaded side of the boat at each station and the depth at which the

211    Secchi disk was no longer visible was recorded (Wetzel and Likens, 2000).

212    Water column samples were collected using a 5 L vertical Niskin bottle (General

213    Oceanics model 1010). Niskin casts were evenly distributed between one or more high-density

214    polyethylene bottles that were rinsed with site water and stored in a cooler. Three to four Niskin

215    casts were used to fill the bottles, such that each bottle is a composite sample of the water

216    collected. Surface samples were taken 0.75 m below the water's surface, mid-column samples

217    were taken at approximately 4.25 m below surface, and benthic or bottom samples were taken

218    at approximately 0.5 m above the lake bottom at each station. Surface samples were taken at

219    all stations while mid-column and benthic sample collection varied between sites and years.

220    Scum samples of dense cyanobacterial accumulation on the surface of the water were collected

221    opportunistically using a 2 L modified Van Dorn water sampler. Sampling times were reported

222    as Eastern Daylight Time (UT -4:00). Upon arrival at the laboratory, raw water samples were

223    immediately subsampled and preserved until analysis.

224          Wind speed and wave height data were obtained from moored buoy continuous

225    monitoring systems in proximity to sampling stations for a timestamp that corresponded to the

226    time samples were collected at that station. Wave height data for all stations were obtained from

227    the Toledo Intake Buoy (owned and maintained by Limnotech Inc.). Wind speed data for

228    stations WE02, WE06, WE09, WE12, WE14, WE15, and WE16 were also collected from this

229    buoy. Data for this buoy is available through the Great Lakes Observing System (GLOS;

230    platform ID 45165, https://seagull.glos.org/data-console/71). Wind speed data for stations

231    WE04, WE08, and WE13 were obtained from the Toledo Harbor Light no. 2 buoy (Station

232    THLO1, owned and maintained by GLERL). Data for this buoy is available through NOAA's

233    National Data Buoy Center (https://www.ndbc.noaa.gov/station_realtime.php?station=THLO1).

234

## Laboratory analysis of samples

236          Water collected from WLE was subsampled to make a range of analytical

237    measurements in the laboratory (Table 2).

238

239   Table 2. Summary of parameters reported in the dataset. Wind speed and wave height data are

240   collected from moored buoy continuous monitoring systems which provide the data in Imperial

241   units.

| Parameter | Years monitored | Method |
|---|---|---|
| Surface samples (n=1296) | 2012-2021 | n/a |
| Mid-column samples (n=19) | 2015 | n/a |
| Benthic samples (n=512) | 2015-2021 | n/a |
| Station depth (m) | 2012-2021 | Sea-Bird 19plus V2 CTD profiler |
| Time of sampling (Eastern Daylight Time UTC -4:00) | 2012-2021 | n/a |
| Latitude (decimal degree) | 2012-2021 | n/a |
| Longitude (decimal degree) | 2012-2021 | n/a |
| Wind speed (knots) | 2015-2021 | Moored buoy continuous monitoring systems |
| Wave height (ft) | 2012-2021 | Moored buoy continuous monitoring systems |
| Cloud cover (sky) | 2012-2021 | Qualitative description |
| Secchi depth (m) | 2012-2021 | Wetzel and Likens (2000) |
| Sample temperature (°C) | 2012 | Vee Gee Scientific digital thermometer |
| CTD temperature (°C) | 2013-2021 | Sea-Bird 19plus V2 CTD profiler |
| CTD specific conductivity ($\mu$S cm$^{-1}$) | 2013-2021 | Sea-Bird 19plus V2 CTD profiler |
| CTD beam attenuation (m$^{-1}$) | 2013-2021 | Sea-Bird 19plus V2 CTD profiler |
| CTD transmission (%) | 2013-2021 | Sea-Bird 19plus V2 CTD profiler |
| CTD dissolved oxygen (DO; mg L$^{-1}$) | 2013-2021 | Sea-Bird 19plus V2 CTD profiler |
| CTD photosynthetically active radiation (PAR; $\mu$E m$^{-2}$ s$^{-1}$) | 2013-2021 | Sea-Bird 19plus V2 CTD profiler |

| | | |
|---|---|---|
| Turbidity (NTU) | 2013-2021 | EPA Method 180.1 |
| Particulate microcystins ($\mu g\ L^{-1}$) | 2012-2021 | Wilson et al. (2008) |
| Dissolved microcystins ($\mu g\ L^{-1}$) | 2014-2021 | Wilson et al. (2008) |
| Phycocyanin ($\mu g\ L^{-1}$) | 2012-2021 | Horvath et al. (2013) |
| Chlorophyll *a* ($\mu g\ L^{-1}$) | 2012-2021 | Speziale et al. (1984) |
| Total phosphorus (TP; $\mu g\ L^{-1}$) | 2012-2021 | Standard Method 4500-P |
| Total dissolved phosphorus (TDP; $\mu g\ L^{-1}$) | 2012-2021 | Standard Method 4500-P |
| Soluble reactive phosphorus (SRP; $\mu g\ L^{-1}$) | 2012-2021 | Standard Method 4500-P |
| Ammonium-N ($\mu g\ L^{-1}$) | 2012-2021 | Standard Method 4500-nh3-nitrogen (    Ammonium) |
| Nitrate-N + Nitrite-N ($mg\ L^{-1}$) | 2012-2021 | Standard Method 4500-no3-nitrogen (nitrate) |
| Urea-N ($\mu g\ L^{-1}$) | 2016-2017 | Milvenna and Savidge (1992), Goeyens et al. (1998), Chaffin and Bridgeman (2014) |
| Particulate organic carbon (POC; $mg\ L^{-1}$) | 2012-2021 | Hedges and Stern (1984) |
| Particulate organic nitrogen (PON; $mg\ L^{-1}$) | 2012-2021 | Hedges and Stern (1984) |
| Colored dissolved organic material (CDOM; $m^{-1}$) | 2014-2021 | Binding et al. (2008), Mitchell et al. (2003) |
| Dissolved organic carbon (DOC; $mg\ L^{-1}$) | 2012-2017 | APHA Standard Method 5310 B |
| Total suspended solids (TSS; $mg\ L^{-1}$) | 2012-2021 | APHA Standard Method 2540 |
| Volatile suspended solids (VSS; $mg\ L^{-1}$) | 2012-2021 | APHA Standard Method 2540 |

242

## Optical properties

244    Turbidity was measured on raw samples using a Hach 2100AN Turbidimeter following

245    US EPA method 180.1 (1993). Colored dissolved organic material (CDOM, also defined as

246    chromophoric dissolved organic matter) was determined by filtering lake water through an acid

247     rinsed 0.2 μm nuclepore polycarbonate filter into acid-washed and combusted borosilicate vials.

248     Optical density of the filtered samples was then measured using a Perkin Elmer UV/VIS

249     Lambda 35 spectrophotometer at wavelengths from 300-800 nm. CDOM absorption was

250     calculated at 400 nm (Mitchell et al., 2003; Binding et al., 2008).

251        Dissolved organic carbon (DOC) concentrations were determined following American

252     Public Health Association (APHA) Standard Method 5310 B. Briefly, lake water was filtered

253     through 0.45 μm polyvinylidene difluoride membrane filters into combusted borosilicate glass

254     vials and frozen at -20°C until analysis. The filtrate was acidified with HCl and sparged with air

255     for 6 min before being analyzed on a Shimadzu total organic carbon analyzer.

256        Duplicate samples for particulate organic carbon (POC) and particulate organic nitrogen

257     (PON) were collected onto pre-combusted glass fiber filters and analyzed following Hedges and

258     Stern (1984) Samples were stored at -20 °C until analysis. The filters were then acidified by

259     fumigation with 10% HCl and dried at 70°C for 24 h before being quantified on a Perkin Elmer

260     2400 or a Carlo-Erba 1110 CHN elemental analyzer.

261        Total suspended solids (TSS) and volatile suspended solids (VSS) were determined via

262     gravimetric analysis following APHA Standard Method 2540. A known volume of lake water was

263     filtered through a pre-combusted, pre-weighed Whatman GF/F glass fiber filter. The filters were

264     then dried at 60° C for at least 24 h and reweighed. The difference in mass between the pre-

265     weighed and processed filter was reported as TSS. Volatile suspended solids concentrations

266     were quantified by combusting the filters used for TSS analysis at 450 °C for 4 h, weighing the

267     combusted filters, and calculating the mass lost.

268     Nutrient fractions

269        Total phosphorus (TP) and total dissolved phosphorus (TDP) samples were collected in

270     duplicate by subsampling 50 mL (2012 to 2019) or 20 mL (2020 to 2021) of lake water into acid

271     washed glass tubes and by filtering 20 mL of lake water through a 0.2 μm membrane filter and

272    collecting the filtrate, respectively. Samples for TP and TDP were refrigerated until samples

273    were digested with potassium persulfate solution and autoclaved at 121°C for 30 min, modified

274    from APHA Standard Method 4500-P. Digested TP and TDP samples were stored at room

275    temperature until concentrations were measured on a Seal QuAAtro continuous segmented flow

276    analyzer (SEAL Analytical Inc.) from 2012 to 2019 and a Seal AA3 from 2020 to 2021 using the

277    ascorbic acid molybdenum method as detailed by the instrument manual and APHA Standard

278    Method 4500-P. Analytical detection limits for the analyses were taken from the instrument

279    manufacturer's documentation.

280          Soluble reactive phosphorus (SRP),     ammonium, nitrate + nitrite, and urea were each

281    determined by filtering 12 mL of lake water through a 0.2 μm membrane filter into 15 mL

282    centrifuge tubes during field sampling. Sample filtrates were stored at -20 °C upon receipt at the

283    laboratory. Soluble reactive phosphorus,     ammonium, and nitrate + nitrite concentrations

284    were determined simultaneously on a Seal AA3 continuous segmented flow analyzer. Soluble

285    reactive phosphorus concentrations, like TP and TDP concentrations, were measured using the

286    ascorbic acid molybdenum method as detailed by the instrument manual and APHA Standard

287    Method 4500-P.    Ammonium concentrations were measured using Bertholet reactions

288    according to the instrument manual and APHA Standard Method 4500-nh3-nitrogen. Nitrate +

289    nitrite concentrations were measured using copper-cadmium reduction methods according to

290    the instrument manual and APHA Standard Method 4500-no3-nitrogen. Analytical detection

291    limits for these inorganic nutrient analyses were taken from the instrument manufacturer's

292    documentation. Urea samples were measured by adding diacetyl monoxime and

293    thiosemicarbazide to the filtrate and briefly vortexing to mix, followed by adding sulfuric acid and

294    ferric chloride to the solution and briefly vortexing to mix. Samples were then incubated in the

295    dark for 72 h at room temperature before absorbance at 520 nm was read on a Perkin Elmer

296    UV/VIS Lambda 35 spectrophotometer. Urea concentrations were then quantified using a

297    standard curve (Mulvenna and Savidge, 1992; Goeyens et al., 1998; Chaffin and Bridgeman,

298    2014). The detection limit was calculated using the standard deviation of repeated

299    measurements.


300        Photopigments and microcystins

301            Particulate phycocyanin and chlorophyll *a* concentrations were determined by filtering a

302    known volume of lake water under low vacuum (<200 mm Hg) onto 47 mm Whatman GF/F

303    glass fiber filters (Cytiva Life Sciences). Particulate phycocyanin sample filters were stored in 15

304    mL conical polypropylene centrifuge tubes and chlorophyll *a* sample filters were stored in amber

305    glass vials at -20 °C until analysis. Analysis methods for particulate phycocyanin were derived

306    from Horváth et al. (2013) where 9 mL of phosphate buffer was added to sample tubes and samples

307    were agitated using a shaker at 5 °C for 15 min at 100 rpm then vortexed for 10 s each. To

308    encourage cell lysis, samples were subjected to three freeze/thaw cycles at -20 °C followed by

309    sonication for 20 min using a Fisher FS110 H sonicator. Fluorescence of the extracted samples was

310    measured using an Aquafluor 8000-010 fluorometer (Turner Designs) with excitation from 400-600

311    nm and emission filter of >595 nm. Particulate phycocyanin was calibrated annually against C-

312    Phycocyanin material from Sigma-Aldrich. Analysis methods for chlorophyll *a* were derived from

313    Speziale et al. (1984) where chlorophyll *a* was extracted from samples using dimethylformamide

314    and placed into a 65 °C water bath for 15 min. Samples were then cooled to room temperature

315    and vortexed for 15-20 s before being quantified using a 10 AU fluorometer (Turner Designs)

316    with excitation filter of 436 nm and emission at 680 nm. Phycocyanin and chlorophyll *a*

317    procedures were performed under low or green light to reduce pigment degradation within the cell.

318            Dissolved and particulate microcystins were quantified using a procedure adapted from

319    Wilson et al. (2008). Dissolved microcystins (dMC) were determined through duplicate samples

320    of ~ 2 mL filtrate that was passed through a 0.2 µm membrane filter and stored in glass vials at -

321    20 °C until analysis. Particulate microcystins (pMC) were collected by filtering a known volume

322    of lake water onto a Whatman GF/F glass fiber filter (2012 to 2015) or a 3 µm pore size

323    polycarbonate membrane filter (2016 to 2021). Particulate MC was then extracted from the

324    filters. In sampling years 2012 to 2015, glass fiber filters were submerged in a glass vial

325    containing a 75:25 methanol:water solution (MeOH/H$_2$O) and sonicated in an ice bath for 2 min.

326    The samples were centrifuged for 15 min and the supernatant was transferred to a clean glass

327    vial. An additional 5 mL of MeOH/H$_2$O was added to the filter/precipitate and the sample was

328    incubated at -20 °C for 5 h. The sample was then sonicated for 2 min, centrifuged, and the

329    supernatant was removed and added to the first extract vial. The composite supernatant was

330    then centrifuged under a vacuum until dry. The dried extract was then stored at -20 °C until

331    analysis. Particulate MC concentrations were then determined by adding 1 mL of MIlliQ water to

332    the sample and using sonication to dissolve the dried extract. For sampling years 2016 to 2021,

333    filters were stored in 2 mL sterile microcentrifuge tubes at -20 °C until analysis. During analysis,

334    pMC were extracted from the membrane filters by adding 1 mL of MilliQ water and subjecting

335    samples to three freeze/thaw cycles at -20 °C followed by addition of Abraxis QuickLyse

336    reagents according to the manufacturer (Eurofins/Abraxis). Particulate MC samples for all

337    sampling years were analyzed immediately after extraction. For all sampling years, dMC and

338    pMC concentrations were determined using a congener-independent enzyme-linked

339    immunosorbent assay (ELISA) kit designed to detect and quantity microcystins and nodularins

340    using the ADDA moiety (Envirologix brand used from 2012 to 2015; Eurofins/Abraxis

341    microcystins/nodularins (ADDA) (EPA ETV) (EPA method 546), ELISA, 96-test kit used from

342    2016 to 2021). Analytical detection limits for the analyses were taken from the manufacturer's

343    documentation.

# Results and Discussion

344

345       This dataset demonstrates the temporal and spatial variability in water quality

346 parameters in western Lake Erie from 2012 to 2021. Overall, sites closest    to the Maumee

347 River inflow (i.e., WE06 and WE09) had the highest median concentrations of nutrients,

348 sediments, pigments, and microcystins compared to sites further out in the basin (i.e., WE02,

349 WE04, and WE13; Table 3). Stations WE06 and WE04 were sampled since the initiation of the

350 monitoring program and consistently represented the high and low extremes of water quality

351 observations during a given time point, respectively, (Table 3) and select parameters for these

352 two sites are represented in figs. 3 and 4. Supplemental figs. 1-16 display the same parameters

353 as figs. 3 and 4 for the remaining stations.

354
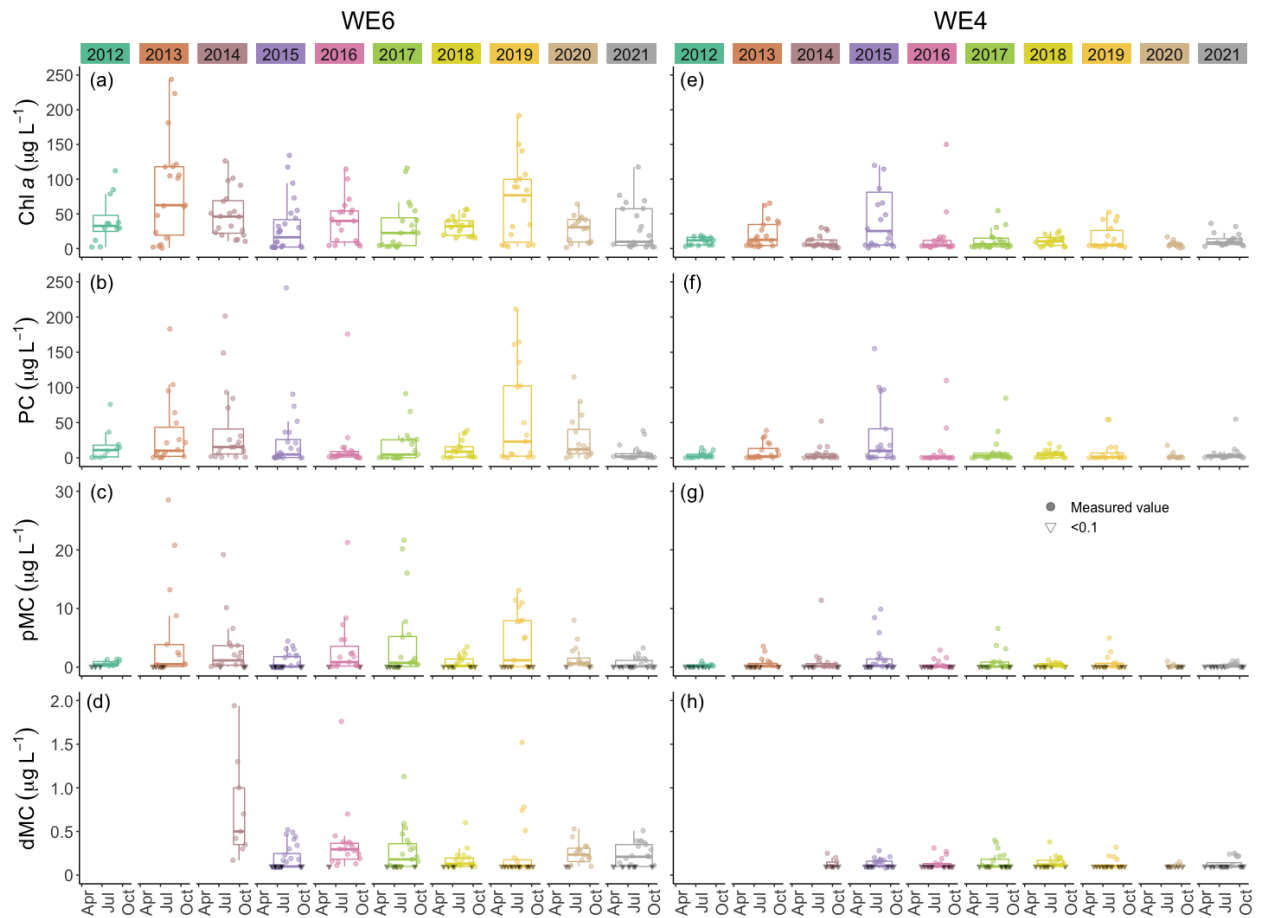
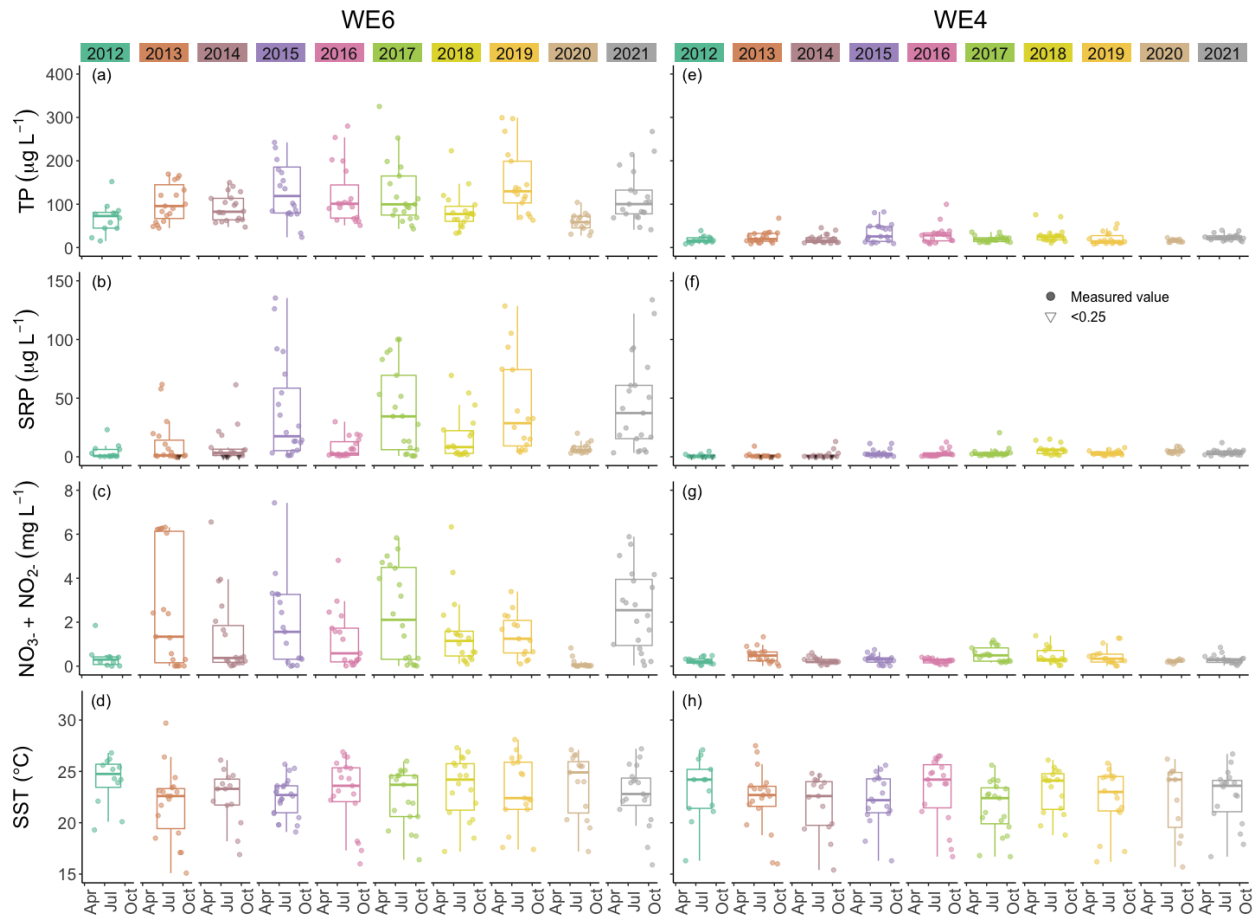Fig 3. Comparison of chlorophyll *a* (Chl *a*), phycocyanin (PC), particulate microcystins (pMC), and dissolved microcystins (dMC) between stations WE04 and WE06 from 2012 to 2021. Boxplots represent the median and 25% and 75% quartiles with whiskers extending to the highest or lowest point within 1.5x the interquartile range. A scatterplot is overlaid on the boxplots.

Fig 4. Comparison of total phosphorus (TP), soluble reactive phosphorus (SRP), nitrate plus nitrite ($NO_3^-$ + $NO_2^-$), and sea surface temperature (SST) between stations WE04 and WE06 from 2012 to 2021. Boxplots represent the median and 25% and 75% quartiles with whiskers extending to the highest or lowest point within 1.5x the interquartile range. A scatterplot is overlaid on the boxplots.

369 Table 3. Median values of each parameter at each monitoring station for all surface samples
370 collected between 2012 to 2021.

| | Secchi depth (m) | Temp. (°C) | Cond. (µS cm⁻¹) | DO (mg L⁻¹) | PAR (µE m⁻² s⁻¹) | Beam Attenuation (m⁻¹) | Transmission (%) | Turbidity (NTU) | Particulate MC (µg L⁻¹) | Dissolved MC (µg L⁻¹) | Phycocyanin (µg L⁻¹) | Chl-a (µg L⁻¹) | TP (µg L⁻¹) | TDP (µg L⁻¹) | SRP (µg L⁻¹) | Ammonia (µg L⁻¹) | Nitrate + Nitrite (mg L⁻¹) | POC (mg L⁻¹) | PON (mg L⁻¹) | CDOM (m⁻¹) |
|------|------|------|------|------|------|------|------|------|------|------|------|------|------|------|------|------|------|------|------|------|
| WE02 | 0.8 | 23.1 | 287 | 7.7 | 264 | 5.1 | 28.2 | 9.9 | 0.78 | 0.20 | 4.8 | 17.5 | 53.3 | 12.8 | 5.7 | 12.6 | 0.44 | 1.4 | 0.23 | 0.99 |
| WE04 | 2.0 | 22.9 | 244 | 7.6 | 377 | 2.2 | 58.4 | 3.0 | 0.46 | 0.17 | 1.2 | 7.7 | 19.2 | 4.5 | 2.2 | 12.9 | 0.27 | 0.63 | 0.10 | 0.34 |
| WE06 | 0.5 | 23.0 | 346 | 7.6 | 173 | 6.4 | 20.5 | 14.8 | 1.5 | 0.28 | 8.0 | 33.0 | 90.1 | 18.7 | 8.7 | 11.8 | 0.83 | 2.4 | 0.38 | 2.0 |
| WE08 | 1.0 | 23.3 | 299 | 7.7 | 166 | 4.3 | 34.4 | 9.0 | 0.88 | 0.22 | 5.7 | 19.5 | 50.9 | 12.3 | 5.8 | 13.8 | 0.45 | 1.5 | 0.25 | 1.1 |
| WE09 | 0.3 | 23.9 | 395 | 7.1 | 127 | 12.6 | 4.3 | 23.2 | 0.95 | 0.26 | 5.2 | 32.6 | 133 | 44.8 | 29.5 | 43.1 | 1.4 | 2.5 | 0.42 | 2.4 |
| WE12 | 0.8 | 23.1 | 276 | 7.7 | 266 | 5.4 | 25.9 | 11.0 | 0.67 | 0.16 | 2.9 | 15.1 | 47.6 | 10.1 | 5.4 | 8.4 | 0.31 | 1.2 | 0.20 | 0.81 |
| WE13 | 1.5 | 22.9 | 244 | 7.8 | 456 | 2.7 | 52.4 | 4.3 | 0.56 | 0.15 | 2.6 | 8.6 | 22.3 | 5.0 | 2.7 | 10.2 | 0.25 | 0.78 | 0.14 | 0.38 |
| WE14 | 1.4 | 23.2 | 238 | 8.1 | 796 | 3.7 | 40.2 | 7.2 | 0.80 | 0.16 | 17.0 | 40.0 | 31.0 | 4.7 | 1.5 | 2.9 | 0.17 | 1.7 | 0.27 | 0.60 |
| WE15 | 1.0 | 23.0 | 261 | 7.7 | 391 | 3.4 | 43.0 | 6.3 | 0.86 | 0.19 | 2.7 | 12.7 | 34.8 | 5.5 | 2.0 | 23.9 | 0.27 | 1.1 | 0.18 | 0.54 |
| WE16 | 1.3 | 24.1 | 269 | 7.4 | 297 | 3.6 | 40.8 | 6.3 | 0.91 | 0.18 | 3.4 | 12.3 | 30.2 | 7.2 | 4.0 | 10.6 | 0.30 | 1.0 | 0.16 | 0.71 |

371

## Physicochemical properties

Median surface temperatures for all samples across all years ranged from 22.9 to 24.1 °C and median benthic temperatures ranged from 22.8 to 23.2 °C (Table 3, Fig. 4), indicating that WLE was thermally well mixed throughout the sampling period. A summary of the dataset indicates that 23.8% of surface temperatures were ≥25 °C, and these higher temperatures all occurred from mid-June through the end of September. Bloom forming cyanobacteria species in Lake Erie, including *Microcystis spp.,* often reach maximum growth rates at warmer temperatures (≥ 25 °C) than eukaryotic phytoplankton (Steffen et al., 2014; Huisman et al., 2018). Despite having warmer temperatures that promote recurring HABs, there was only one recorded instance of hypoxia (DO <2 mg L$^{-1}$) in the dataset and it occurred at WE13 on 08 July 2019. Median DO was 7.62 mg L$^{-1}$ in all surface samples and 7.02 mg L$^{-1}$ in all benthic samples from 2012 to 2021 (Table 3), again indicating minimal stratification in WLE during sampling. Median conductivity from 2012 to 2021 was highest at sites WE06 and WE09, which are closest to the Maumee River input, and lowest at sites WE04 and WE13 near the middle of the basin (Table 3). WE06 and WE09 were the only sites to have median conductivity values above 300 µS cm$^{-1}$.

## Optical properties

Biotic and abiotic particulate concentrations and movement patterns in WLE are prone to spatial and seasonal variations and are heavily influenced by loading from the Maumee River (Prater et al., 2017; Maguire et al., 2022). Secchi depth, turbidity, and PAR measurements have been correlated with distance from Maumee Bay, where light penetration was lowest near the Maumee River (Chaffin et al., 2011). Variability in optical property measurements in WLE is also dependent on Maumee River inputs, and changes in optical properties can potentially be used

395    in remote sensing algorithms to detect changes in water quality (Sayers et al., 2019). Median

396    Secchi disk depth over the entire dataset was highest at WE04 and lowest at WE06 and WE09,

397    which are closest to the Maumee River (Table 3). Other optical properties, such as PAR, beam

398    attenuation, and transmittance also followed this spatial pattern. In a summary of all samples,

399    median PAR measured at 0.5 m below surface was highest at WE13 and WE14 and lowest at

400    WE09; median transmittance was highest at WE04 and lowest at WE09; and median beam

401    attenuation and turbidity were highest at WE09 and lowest at WE04 (Table 3). Median turbidity

402    values at each site over the 2012 to 2021 period were within the range of previously reported

403    values in the WLE basin (Barbiero and Tuchman, 2004). Median CDOM absorbance and DOC,

404    TSS, and VSS concentrations were again highest at WE09 and lowest at WE04 (Table 3).

405    CDOM gradients in WLE are likewise affected by loading from the Maumee River (Cory et al.,

406    2016) and DOC and CDOM values from this dataset have been used as predictor variables in

407    models estimating PAR attenuation variation in WLE (Weiskerger et al., 2018).


## Nutrient fractions

409         The Maumee River is a major contributor of nutrients to Lake Erie (Steffen et al., 2014;

410    Kast et al., 2021). Median TP concentrations in WLE from 2012 to 2021 were lowest at WE04

411    and highest at WE09 (Table 3, Fig. 4). Median concentrations at each station from 2012 to 2021

412    were above the GLWQA Annex 4 goals for TP concentration in open waters, which is 15 µg P L$^{-}$

413    $^{1}$ for WLE. This goal was met in 92 of 1275 (7.2%) samples and these target values were

414    primarily recorded from stations WE04 and WE13. Sites closer to the mouth of the Maumee

415    River had higher median TP values. While TP loading from the Maumee River tributary declined

416    between 1982 to 2018 (Rowland et al., 2020) the proportion of dissolved P has increased

417    (Joosse and Baker, 2011; Stow et al., 2015). Median TDP values in the WLE dataset were

418    lowest at WE04 and highest at WE09 (Table 3) with a highest recorded value of 274 µg P L$^{-1}$ at

419    WE08 in 2015. Median SRP concentrations for each station in this dataset were lowest at WE14

420    and WE15 and were highest at WE09 (Table 3). The maximum recorded SRP concentration

421    was 135.4 µg P L$^{-1}$ at WE06 in 2015 (Fig. 4). Using this dataset, Newell et al. (2019) found that

422    the Maumee River N loading has become more chemically reduced over time where ammonium

423    and PON have increased. Median     ammonium concentrations in WLE from 2012 to 2019

424    were lowest at WE12 and WE14 and highest at WE09 (Table 3) with a recorded maximum

425    concentration of 2109 µg N L$^{-1}$ at WE12 in 2017. Median nitrate + nitrite was lowest at WE13

426    and WE14 and highest at WE09 (Table 3), with a maximum recorded value of 9.5 mg N L$^{-1}$ at

427    WE09 in 2016. See Fig. 4 for a comparison of nitrate + nitrite concentrations between WE04

428    and WE06. Median PON concentrations were lowest at WE04 and highest at WE09 (Table 3)

429    with a recorded max of 40.93 mg N L$^{-1}$ at WE08 in 2015.


430    # Photop     igments and microcystins


431        Median extracted chlorophyll *a* concentrations in surface waters from 2012 to 2021 were

432    lowest at WE04 and highest at WE06 (Table 3, Fig. 3). The highest recorded surface

433    concentration of chlorophyll *a* was 6784 µg L$^{-1}$ on 10 August 2015 at WE08 during the most

434    severe bloom year in this dataset, according to the CI Index (Wynne et al., 2013; Lunetta et al.,

435    2015). The highest measured levels of particulate phycocyanin, pMC, and TP were also

436    recorded at WE06 on 10 August 2015. Other notably high chlorophyll *a* concentrations were

437    measured during severe bloom years in 2017 (532 µg L$^{-1}$ at WE09 on 04 August) and 2019 (593

438    µg L$^{-1}$ at WE09 on 05 August). Similarly, median surface particulate phycocyanin concentration

439    for 2012 to 2021 was highest at WE06 and lowest at WE04 (Table 3, Fig. 4). The highest

440    recorded phycocyanin value was from WE08 on 10 August 2015 (8228 µg L$^{-1}$), followed by 3315

441    µg L$^{-1}$ at WE06 in 2013 during another severe bloom year.

442     Particulate MC concentrations had highest median concentrations at WE06 and were

443     lowest at WE04 (Table 3, Fig. 4), similar to particulate chlorophyll *a* and phycocyanin

444     observations. The highest recorded particulate MC concentration in this dataset was from 10

445     August 2015 at WE08 during a severe bloom year (297 µg L$^{-1}$), followed by 289 µg L$^{-1}$ at WE06

446     in 2017 during another severe bloom year according to the CI Index (Wynne et al., 2013;

447     Lunetta et al., 2015). Median dMC concentrations were highest at WE06 and lowest at WE13

448     (Table 3). The maximum dissolved MC in the dataset was 8.19 µg L$^{-1}$ at WE09 on 05 August

449     2019, which correlates with high chlorophyll *a* concentrations.

450     Although the United States does not federally enforce water quality criteria or regulations

451     for cyanotoxins in drinking water, the US EPA has a recommended health advisory of 1.6 µg L$^{-1}$

452     microcystins in drinking water for school-age children through adults (US EPA, 2015) while the

453     WHO and the Ohio EPA use 1 µg L$^{-1}$ microcystins as a guideline (WHO, 2020). From 2012 to

454     2021, 44.4% of pMC samples in this dataset exceeded the WHO guidelines and 34.1%

455     exceeded the US EPA health advisory. Monitoring MC concentrations in western Lake Erie has

456     become especially pertinent since August 2014 when the Toledo, OH drinking water treatment

457     plant was contaminated with microcystins in excess of 1 µg L$^{-1}$ and customers were alerted to

458     not drink their tap water until toxin levels were decreased (Steffen et al., 2017). The pMC

459     concentrations at our WLE monitoring stations varied from 1.2-10.1 µg L$^{-1}$ on 04 August 2014

460     during this crisis.

461

# Data Availability

463        The entire dataset detailed in this manuscript can be freely accessed through the NOAA

464    National Centers for Environmental Information (NCEI) data repository at

465    https://www.ncei.noaa.gov/. The data collection is titled "Physical, chemical, and biological water

466    quality monitoring data to support detection of Harmful Algal Blooms (HABs) in western Lake

467    Erie, collected by the Great Lakes Environmental Research Laboratory and the Cooperative

468    Institute for Great Lakes Research since 2012". The digital object identifier is

469    https://doi.org/10.25921/11da-3x54. The data presented in this manuscript are available in three

470    separate accession files within this collection including: 2012 to 2018 data is available under

471    NCEI Accession 0187718 v2.2 at https://www.ncei.noaa.gov/archive/accession/0187718; 2019

472    data is available under NCEI Accession 0209116 v1.1 at

473    https://www.ncei.noaa.gov/archive/accession/0209116; 2020 to 2021 data is available under

474    NCEI Accession 0254720 v1.1 at https://www.ncei.noaa.gov/archive/accession/0254720

475    (Cooperative Institute for Great Lakes Research, University of Michigan; NOAA Great Lakes

476    Environmental Research Laboratory, 2019). Future data will be added to this collection as it

477    becomes available.

# Conclusions

478

479       The western Lake Erie data collected and compiled by NOAA GLERL and CIGLR

480    represent ten years of routine water quality monitoring to detect, track, and predict

481    cyanobacterial HAB events in an area of the Great Lakes that has experienced significant

482    environmental degradation.     This ongoing program provides a service to the region and

483    contributes data for investigating the nuanced dynamics of potentially toxic HABs fueled by

484    excess nutrient loading into the WLE basin.

485       In addition to serving the need for generating data to improve remote sensing efforts,

486    (see: Sayers et al., 2016, 2019; Stumpf et al., 2016; Avouris and Ortiz, 2019; Bosse et al., 2019;

487    Vander Woude et al., 2019; Pirasteh et al., 2020; Xu et al., 2022) this monitoring program will

488    continue to serve stakeholders and communities in the Laurentian Great Lakes. As this program

489    has grown, so too has the scope of application of its dataset. For instance, this dataset has

490    assisted in assessing progress toward binational nutrient loading reduction efforts on lake basin

491    concentrations of phosphorus. It has also been used towards determining the significance of

492    nitrogen in bloom formation and toxicity (Gobler et al., 2016; Newell et al., 2019; Hoffman et al.,

493    2022). Other research groups have taken advantage of this dataset to investigate microbial and

494    algal community dynamics (Berry et al., 2017; Kharbush et al., 2019; Smith et al., 2021; Marino

495    et al., 2022; Smith et al., 2022), the genomic diversity of cyanobacteria in the WLE basin

496    (Yancey et al., 2022), and hydrogen peroxide production and dynamics within blooms (Corey et

497    al., 2016; Pandey et al., 2022). We anticipate this dataset will continue to be useful for

498    addressing the complex relationships of abiotic and biotic factors contributing to WLE HABs.

499    Long-term monitoring programs like this one provide consistent data which is useful for

500    identifying patterns and variations within the ecosystem and in determining the root cause of

501    those changes.

502     As the sites and parameters of this monitoring program have already changed to adapt

503     to the needs of research, this program will continue to evolve as we consider adding parameters

504     that encompass     broader aspects of bloom dynamics. For example, lake samples can be

505     analyzed for genomic data that will provide insights on the ability of the current phytoplankton

506     community to produce microcystins. This decadal history has already been an invaluable

507     resource for the research community, and it will continue to enrich our collective scientific

508     knowledge of water quality dynamics in western Lake Erie.

# Acknowledgements

# Author Contributions

519

520 Anna G Boegehold prepared the manuscript. Ashley M. Burtner performed field sampling,

521 laboratory processing, data processing, QA/QC and data management, manuscript revision,

522 data curation. Andrew Camilleri performed field sampling, laboratory processing, manuscript

523 revision. Glenn Carter performed field sampling, laboratory processing, data processing,

524 methodology. Paul DenUyl performed field sampling, laboratory processing, manuscript

525 revision. David Fanslow performed field sampling, laboratory processing. Deanna Fyffe

526 Semenyuk performed field sampling, laboratory processing, manuscript revision. Casey Godwin

527 was responsible for project administration, supervision, visualization, manuscript revision,

528 methodology, field sampling, sample processing. Duane Gossiaux performed field sampling,

529 laboratory processing, manuscript revision, methodology. Tom Johengen was responsible for

530 project administration, supervision, field sampling, methodology. Holly Kelchner performed field

531 sampling, laboratory processing, manuscript revision. Christine Kitchens performed field

532 sampling, laboratory processing, data processing, manuscript revision. Lacey A. Mason was

533 responsible for data curation, manuscript revision. Kelly McCabe performed field sampling,

534 laboratory processing, manuscript revision, methodology. Danna Palladino performed field

535 sampling, laboratory processing, data processing, manuscript revision. Dack Stuart performed

536 field sampling, data processing. Henry Vanderploeg was responsible for project administration,

537 supervision. Reagan Errera was responsible for project administration, supervision,

538 Visualization, manuscript revision, methodology.

539

# 540 Competing Interests

541 The authors declare that they have no conflict of interest

# References

543  Allinger, L. E. and Reavie, E. D.: The ecological history of Lake Erie as recorded by the
544  phytoplankton community, J. Gt. Lakes Res., 39, 365–382,
545  https://doi.org/10.1016/j.jglr.2013.06.014, 2013.

546  Avouris, D. M. and Ortiz, J. D.: Validation of 2015 Lake Erie MODIS image spectral
547  decomposition using visible derivative spectroscopy and field campaign data, J. Gt. Lakes Res.,
548  45, 466–479, https://doi.org/10.1016/j.jglr.2019.02.005, 2019.

549  Baker, D. B., Ewing, D. E., Johnson, L. T., Kramer, J. W., Merryfield, B. J., Confesor, R. B.,
550  Peter Richards, R., and Roerdink, A. A.: Lagrangian analysis of the transport and processing of
551  agricultural runoff in the lower Maumee River and Maumee Bay, J. Gt. Lakes Res., 40, 479–
552  495, https://doi.org/10.1016/j.jglr.2014.06.001, 2014a.

553  Baker, D. B., Confesor, R., Ewing, D. E., Johnson, L. T., Kramer, J. W., and Merryfield, B. J.:
554  Phosphorus loading to Lake Erie from the Maumee, Sandusky and Cuyahoga rivers: The
555  importance of bioavailability, J. Gt. Lakes Res., 40, 502–517,
556  https://doi.org/10.1016/j.jglr.2014.05.001, 2014b.

557  Barbiero, R. P. and Tuchman, M. L.: Long-term Dreissenid Impacts on Water Clarity in Lake
558  Erie, J. Gt. Lakes Res., 30, 557–565, https://doi.org/10.1016/S0380-1330(04)70371-8, 2004.

559  Berry, M. A., Davis, T. W., Cory, R. M., Duhaime, M. B., Johengen, T. H., Kling, G. W., Marino,
560  J. A., Den Uyl, P. A., Gossiaux, D., Dick, G. J., and Denef, V. J.: Cyanobacterial harmful algal
561  blooms are a biological disturbance to Western Lake Erie bacterial communities, Environ.
562  Microbiol., 19, 1149–1162, https://doi.org/10.1111/1462-2920.13640, 2017.

563  Bertani, I., Steger, C. E., Obenour, D. R., Fahnenstiel, G. L., Bridgeman, T. B., Johengen, T. H.,
564  Sayers, M. J., Shuchman, R. A., and Scavia, D.: Tracking cyanobacteria blooms: Do different
565  monitoring approaches tell the same story?, Sci. Total Environ., 575, 294–308,
566  https://doi.org/10.1016/j.scitotenv.2016.10.023, 2017.

567  Binding, C. E., Jerome, J. H., Bukata, R. P., and Booty, W. G.: Spectral absorption properties of
568  dissolved and particulate matter in Lake Erie, Remote Sens. Environ., 112, 1702–1711,
569  https://doi.org/10.1016/j.rse.2007.08.017, 2008.

570  Bosse, K. R., Sayers, M. J., Shuchman, R. A., Fahnenstiel, G. L., Ruberg, S. A., Fanslow, D. L.,
571  Stuart, D. G., Johengen, T. H., and Burtner, A. M.: Spatial-temporal variability of in situ
572  cyanobacteria vertical structure in Western Lake Erie: Implications for remote sensing
573  observations, J. Gt. Lakes Res., 45, 480–489, https://doi.org/10.1016/j.jglr.2019.02.003, 2019.

574  Bridoux, M., Sobiechowska, M., Perez-Fuentetaja, A., and Alben, K. T.: Algal pigments in Lake
575  Erie dreissenids, pseudofeces and sediments, as tracers of diet, selective feeding and
576  bioaccumulation, J. Gt. Lakes Res., 36, 437–447, https://doi.org/10.1016/j.jglr.2010.06.005,
577  2010.

578  Buratti, F. M., Manganelli, M., Vichi, S., Stefanelli, M., Scardala, S., Testai, E., and Funari, E.:
579  Cyanotoxins: producing organisms, occurrence, toxicity, mechanism of action and human health

580    toxicological risk evaluation, Arch. Toxicol., 91, 1049–1130, https://doi.org/10.1007/s00204-016-
581    1913-6, 2017.

582    Carmichael, W. W. and Boyer, G. L.: Health impacts from cyanobacteria harmful algae blooms:
583    Implications for the North American Great Lakes, Harmful Algae, 54, 194–212,
584    https://doi.org/10.1016/j.hal.2016.02.002, 2016.

585    Chaffin, J. D. and Bridgeman, T. B.: Organic and inorganic nitrogen utilization by nitrogen-
586    stressed cyanobacteria during bloom conditions, J. Appl. Phycol., 26, 299–309,
587    https://doi.org/10.1007/s10811-013-0118-0, 2014.

588    Chaffin, J. D., Bridgeman, T. B., Heckathorn, S. A., and Mishra, S.: Assessment of Microcystis
589    growth rate potential and nutrient status across a trophic gradient in western Lake Erie, J. Gt.
590    Lakes Res., 37, 92–100, https://doi.org/10.1016/j.jglr.2010.11.016, 2011.

591    Charlton, M. N., Milne, J. E., Booth, W. G., and Chiocchio, F.: Lake Erie Offshore in 1990:
592    Restoration and Resilience in the Central Basin, J. Gt. Lakes Res., 19, 291–309,
593    https://doi.org/10.1016/S0380-1330(93)71218-6, 1993.

594    Conroy, J. D., Kane, D. D., Dolan, D. M., Edwards, W. J., Charlton, M. N., and Culver, D. A.:
595    Temporal Trends in Lake Erie Plankton Biomass: Roles of External Phosphorus Loading and
596    Dreissenid Mussels, J. Gt. Lakes Res., 31, 89–110, https://doi.org/10.1016/S0380-
597    1330(05)70307-5, 2005.

598    Cooperative Institute for Great Lakes Research, University of Michigan; NOAA Great Lakes
599    Environmental Research Laboratory: Physical, chemical, and biological water quality monitoring
600    data to support detection of Harmful Algal Blooms (HABs) in western Lake Erie, collected by the
601    Great Lakes Environmental Research Laboratory and the Cooperative Institute for Great Lakes
602    Research since 2012, NOAA National Centers for Environmental Information [data set],
603    https://doi.org/10.25921/11da-3x54, 2019.

604    Cory, R. M., Davis, T. W., Dick, G. J., Johengen, T., Denef, V. J., Berry, M. A., Page, S. E.,
605    Watson, S. B., Yuhas, K., and Kling, G. W.: Seasonal Dynamics in Dissolved Organic Matter,
606    Hydrogen Peroxide, and Cyanobacterial Blooms in Lake Erie, Front. Mar. Sci., 3, 2016.

607    Cousino, L. K., Becker, R. H., and Zmijewski, K. A.: Modeling the effects of climate change on
608    water, sediment, and nutrient yields from the Maumee River watershed, J. Hydrol. Reg. Stud., 4,
609    762–775, https://doi.org/10.1016/j.ejrh.2015.06.017, 2015.

610    Den Uyl, P. A., Harrison, S. B., Godwin, C. M., Rowe, M. D., Strickler, J. R., and Vanderploeg,
611    H. A.: Comparative analysis of Microcystis buoyancy in western Lake Erie and Saginaw Bay of
612    Lake Huron, Harmful Algae, 108, 102102, https://doi.org/10.1016/j.hal.2021.102102, 2021.

613    Den Uyl, P. A., Thompson, L. R., Errera, R. M., Birch, J. M., Preston, C. M., Ussler, W. I.,
614    Yancey, C. E., Chaganti, S. R., Ruberg, S. A., Doucette, G. J., Dick, G. J., Scholin, C. A., and
615    Goodwin, K. D.: Lake Erie field trials to advance autonomous monitoring of cyanobacterial
616    harmful algal blooms, Front. Mar. Sci., 9, https://doi.org/10.3389/fmars.2022.1021952, 2022.

617    Dolan, D. M. and Chapra, S. C.: Great Lakes total phosphorus revisited: 1. Loading analysis
618    and update (1994–2008), J. Gt. Lakes Res., 38, 730–740,
619    https://doi.org/10.1016/j.jglr.2012.10.001, 2012.

620 Environment and Climate Change Canada and the U.S. Environmental Protection Agency.
621 2022. State of the Great Lakes 2022 Technical Report. Cat No. En161-3/1E-PDF. EPA 905-
622 R22-004. Available at binational.net, 2022.

623 Fang, S., Del Giudice, D., Scavia, D., Binding, C. E., Bridgeman, T. B., Chaffin, J. D., Evans, M.
624 A., Guinness, J., Johengen, T. H., and Obenour, D. R.: A space-time geostatistical model for
625 probabilistic estimation of harmful algal bloom biomass and areal extent, Sci. Total Environ.,
626 695, 133776, https://doi.org/10.1016/j.scitotenv.2019.133776, 2019.

627 Goeyens, L., Kindermans, N., Abu Yusuf, M., and Elskens, M.: A Room Temperature Procedure
628 for the Manual Determination of Urea in Seawater, Estuar. Coast. Shelf Sci., 47, 415–418,
629 https://doi.org/10.1006/ecss.1998.0357, 1998.

630 Hartig, J. H., Zarull, M. A., Ciborowski, J. J. H., Gannon, J. E., Wilke, E., Norwood, G., and
631 Vincent, A. N.: Long-term ecosystem monitoring and assessment of the Detroit River and
632 Western Lake Erie, Environ. Monit. Assess., 158, 87–104, https://doi.org/10.1007/s10661-008-
633 0567-0, 2009.

634 GLWQA: Great Lakes Water Quality Agreement; Protocol Amending the Agreement Between
635 Canada and the United States of America on Great Lakes Water Quality, 1978, as Amended on
636 October 16, 1983 and on November 18, 1987, https://binational. net/2012/09/05/2012-glwqa-
637 aqegl/ (last access: November 2022), 2012.
638
639 Gobler, C. J., Burkholder, J. M., Davis, T. W., Harke, M. J., Johengen, T., Stow, C. A., and Van
640 de Waal, D. B.: The dual role of nitrogen supply in controlling the growth and toxicity of
641 cyanobacterial blooms, Harmful Algae, 54, 87–97, https://doi.org/10.1016/j.hal.2016.01.010,
642 2016.
643
644 Hartig, J. H., Francoeur, S. N., Ciborowski, J. J. H., Gannon, J. E., Sanders, C. E., Galvao-
645 Ferreira, P., Knauss, C. R., Gell, G., and Berk, K.: An ecosystem health assessment of the
646 Detroit River and western Lake Erie, J. Gt. Lakes Res., 47, 1241–1256,
647 https://doi.org/10.1016/j.jglr.2021.05.008, 2021.

648 Hedges, J. I. and Stern, J. H.: Carbon and nitrogen determinations of carbonate-containing
649 solids1, Limnol. Oceanogr., 29, 657–663, https://doi.org/10.4319/lo.1984.29.3.0657, 1984.

650 Hellweger, F. L., Martin, R. M., Eigemann, F., Smith, D. J., Dick, G. J., and Wilhelm, S. W.:
651 Models predict planned phosphorus load reduction will make Lake Erie more toxic, Science,
652 376, 1001–1005, https://doi.org/10.1126/science.abm6791, 2022.

653 Hoffman, D. K., McCarthy, M. J., Boedecker, A. R., Myers, J. A., and Newell, S. E.: The role of
654 internal nitrogen loading in supporting non-N-fixing harmful cyanobacterial blooms in the water
655 column of a large eutrophic lake, Limnol. Oceanogr., n/a, https://doi.org/10.1002/lno.12185,
656 2022.

657 Horváth, H., Kovács, A. W., Riddick, C., and Présing, M.: Extraction methods for phycocyanin
658 determination in freshwater filamentous cyanobacteria and their application in a shallow lake,
659 Eur. J. Phycol., 48, 278–286, https://doi.org/10.1080/09670262.2013.821525, 2013.

660 Huisman, J., Codd, G. A., Paerl, H. W., Ibelings, B. W., Verspagen, J. M. H., and Visser, P. M.:
661 Cyanobacterial blooms | Nature Reviews Microbiology, Nat. Rev. Microbiol., 16, 471–483,
662 https://doi.org/10.1038/s41579-018-0040-1, 2018.

663 Joosse, P. J. and Baker, D. B.: Context for re-evaluating agricultural source phosphorus
664 loadings to the Great Lakes, Can. J. Soil Sci., 91, 317–327, https://doi.org/10.4141/cjss10005,
665 2011.

666 Kane, D. D., Ludsin, S. A., Briland, R. D., Culver, D. A., and Munawar, M.: Ten+years gone:
667 Continued degradation of offshore planktonic communities in U.S. waters of Lake Erie's western
668 and central basins (2003–2013), J. Gt. Lakes Res., 41, 930–933,
669 https://doi.org/10.1016/j.jglr.2015.06.002, 2015.

670 Kast, J. B., Apostel, A. M., Kalcic, M. M., Muenich, R. L., Dagnew, A., Long, C. M., Evenson, G.,
671 and Martin, J. F.: Source contribution to phosphorus loads from the Maumee River watershed to
672 Lake Erie, J. Environ. Manage., 279, 111803, https://doi.org/10.1016/j.jenvman.2020.111803,
673 2021.

674 Kharbush, J. J., Smith, D. J., Powers, M., Vanderploeg, H. A., Fanslow, D., Robinson, R. S.,
675 Dick, G. J., and Pearson, A.: Chlorophyll nitrogen isotope values track shifts between
676 cyanobacteria and eukaryotic algae in a natural phytoplankton community in Lake Erie, Org.
677 Geochem., 128, 71–77, https://doi.org/10.1016/j.orggeochem.2018.12.006, 2019.

678 Kharbush, J. J., Robinson, R. S., and Carter, S. J.: Patterns in sources and forms of nitrogen in
679 a large eutrophic lake during a cyanobacterial harmful algal bloom, Limnol. Oceanogr., n/a,
680 https://doi.org/10.1002/lno.12311, 2023.

681 King, W. M., Curless, S. E., and Hood, J. M.: River phosphorus cycling during high flow may
682 constrain Lake Erie cyanobacteria blooms, Water Res., 222, 118845,
683 https://doi.org/10.1016/j.watres.2022.118845, 2022.

684 Liu, Q., Rowe, M. D., Anderson, E. J., Stow, C. A., Stumpf, R. P., and Johengen, T. H.:
685 Probabilistic forecast of microcystin toxin using satellite remote sensing, in situ observations and
686 numerical modeling, Environ. Model. Softw., 128, 104705,
687 https://doi.org/10.1016/j.envsoft.2020.104705, 2020.

688 Lunetta, R. S., Schaeffer, B. A., Stumpf, R. P., Keith, D., Jacobs, S. A., and Murphy, M. S.:
689 Evaluation of cyanobacteria cell count detection derived from MERIS imagery across the
690 eastern USA, Remote Sens. Environ., 157, 24–34, https://doi.org/10.1016/j.rse.2014.06.008,
691 2015.

692 Maguire, T. J., Stow, C. A., and Godwin, C. M.: Spatially referenced Bayesian state-space
693 model of total phosphorus in western Lake Erie, Hydrol. Earth Syst. Sci., 26, 1993–2017,
694 https://doi.org/10.5194/hess-26-1993-2022, 2022.

695 Makarewicz, J. C. and Bertram, P.: Evidence for the Restoration of the Lake Erie Ecosystem:
696 Water quality, oxygen levels, and pelagic function appear to be improving, BioScience, 41, 216–
697 223, https://doi.org/10.2307/1311411, 1991.

698 Marino, J. A., Denef, V. J., Dick, G. J., Duhaime, M. B., and James, T. Y.: Fungal community
699 dynamics associated with harmful cyanobacterial blooms in two Great Lakes, J. Gt. Lakes Res.,
700 48, 1021–1031, https://doi.org/10.1016/j.jglr.2022.05.007, 2022.

701 Matisoff, G., Kaltenberg, E. M., Steely, R. L., Hummel, S. K., Seo, J., Gibbons, K. J.,
702 Bridgeman, T. B., Seo, Y., Behbahani, M., James, W. F., Johnson, L. T., Doan, P., Dittrich, M.,
703 Evans, M. A., and Chaffin, J. D.: Internal loading of phosphorus in western Lake Erie, J. Gt.
704 Lakes Res., 42, 775–788, https://doi.org/10.1016/j.jglr.2016.04.004, 2016.

705 Michalak, A. M., Anderson, E. J., Beletsky, D., Boland, S., Bosch, N. S., Bridgeman, T. B.,
706 Chaffin, J. D., Cho, K., Confesor, R., Daloğlu, I., DePinto, J. V., Evans, M. A., Fahnenstiel, G. L.,
707 He, L., Ho, J. C., Jenkins, L., Johengen, T. H., Kuo, K. C., LaPorte, E., Liu, X., McWilliams, M.
708 R., Moore, M. R., Posselt, D. J., Richards, R. P., Scavia, D., Steiner, A. L., Verhamme, E.,
709 Wright, D. M., and Zagorski, M. A.: Record-setting algal bloom in Lake Erie caused by
710 agricultural and meteorological trends consistent with expected future conditions, Proc. Natl.
711 Acad. Sci., 110, 6448–6452, https://doi.org/10.1073/pnas.1216006110, 2013.

712 Mitchell, B.G., Kahru, M., Wieland, J., and Stramska, M.: Determination of spectral absorption
713 coefficients of particles, dissolved material and phytoplankton for discrete water samples, In:
714 Mueller, J.L., G.S. Fargion, and C.R. McClain [Eds.] Ocean Optics Protocols for Satellite Ocean
715 Color Sensor Validation, Revision 4, Volume IV: Inherent Optical Properties: Instruments,
716 Characterizations, Field Measurements and Data Analysis Protocols. NASA/TM- 2003-211621,
717 NASA Goddard Space Flight Center, Greenbelt, MD, Chapter 4, pp 39-64, 2003.

718 Mohamed, M. N., Wellen, C., Parsons, C. T., Taylor, W. D., Arhonditsis, G., Chomicki, K. M.,
719 Boyd, D., Weidman, P., Mundle, S. O. C., Cappellen, P. V., Sharpley, A. N., and Haffner, D. G.:
720 Understanding and managing the re-eutrophication of Lake Erie: Knowledge gaps and research
721 priorities, Freshw. Sci., 38, 675–691, https://doi.org/10.1086/705915, 2019.

722 Mulvenna, P. F. and Savidge, G.: A modified manual method for the determination of urea in
723 seawater using diacetylmonoxime reagent, Estuar. Coast. Shelf Sci., 34, 429–438,
724 https://doi.org/10.1016/S0272-7714(05)80115-5, 1992.

725 Myers, D.N., Thomas, M.A., Frey, J.W., Rheaume, S.J., and Button, D.T.: Water Quality in the
726 Lake Erie-Lake Saint Clair Drainages Michigan, Ohio, Indiana, New York, and Pennsylvania,
727 1996–98: U.S. Geological Survey Circular 1203, 35 p., https://pubs.water.usgs.gov/circ1203/,
728 2000.
729

730 NCWQR: Heidelberg Tributary Loading Program (HTLP) Dataset. Zenodo.
731 https://doi.org/10.5281/zenodo.6606949, 2022.

732 Newell, S. E., Davis, T. W., Johengen, T. H., Gossiaux, D., Burtner, A., Palladino, D., and
733 McCarthy, M. J.: Reduced forms of nitrogen are a driver of non-nitrogen-fixing harmful
734 cyanobacterial blooms and toxicity in Lake Erie, Harmful Algae, 81, 86–93,
735 https://doi.org/10.1016/j.hal.2018.11.003, 2019.

736 Pandey, D. R., Polik, C., and Cory, R. M.: Controls on the photochemical production of
737 hydrogen peroxide in Lake Erie, Environ. Sci.: Processes Impacts, 10.1039.D2EM00327A,
738 https://doi.org/10.1039/D2EM00327A, 2022.

739 Pirasteh, S., Mollaee, S., Fatholahi, S. N., and Li, J.: Estimation of Phytoplankton Chlorophyll-a
740 Concentrations in the Western Basin of Lake Erie Using Sentinel-2 and Sentinel-3 Data, Can. J.
741 Remote Sens., 46, 585–602, https://doi.org/10.1080/07038992.2020.1823825, 2020.

742 Prater, C., Frost, P. C., Howell, E. T., Watson, S. B., Zastepa, A., King, S. S. E., Vogt, R. J., and
743 Xenopoulos, M. A.: Variation in particulate C : N : P stoichiometry across the Lake Erie
744 watershed from tributaries to its outflow, Limnol. Oceanogr., 62, S194–S206,
745 https://doi.org/10.1002/lno.10628, 2017.

746 Qian, S. S., Stow, C. A., Rowland, F. E., Liu, Q., Rowe, M. D., Anderson, E. J., Stumpf, R. P.,
747 and Johengen, T. H.: Chlorophyll a as an indicator of microcystin: Short-term forecasting and
748 risk assessment in Lake Erie, Ecol. Indic., 130, 108055,
749 https://doi.org/10.1016/j.ecolind.2021.108055, 2021.

750 Reavie, E. D., Cai, M., Twiss, M. R., Carrick, H. J., Davis, T. W., Johengen, T. H., Gossiaux, D.,
751 Smith, D. E., Palladino, D., Burtner, A., and Sgro, G. V.: Winter–spring diatom production in
752 Lake Erie is an important driver of summer hypoxia, J. Gt. Lakes Res., 42, 608–618,
753 https://doi.org/10.1016/j.jglr.2016.02.013, 2016.

754 Rowe, M. D., Anderson, E. J., Wynne, T. T., Stumpf, R. P., Fanslow, D. L., Kijanka, K.,
755 Vanderploeg, H. A., Strickler, J. R., and Davis, T. W.: Vertical distribution of buoyant Microcystis
756 blooms in a Lagrangian particle tracking model for short-term forecasts in Lake Erie, J.
757 Geophys. Res. Oceans, 121, 5296–5314, https://doi.org/10.1002/2016JC011720, 2016.

758 Rowland, F. E., Stow, C. A., Johengen, T. H., Burtner, A. M., Palladino, D., Gossiaux, D. C.,
759 Davis, T. W., Johnson, L. T., and Ruberg, S.: Recent Patterns in Lake Erie Phosphorus and
760 Chlorophyll a Concentrations in Response to Changing Loads, Environ. Sci. Technol., 54, 835–
761 841, https://doi.org/10.1021/acs.est.9b05326, 2020.

762 Sayers, M., Fahnenstiel, G. L., Shuchman, R. A., and Whitley, M.: Cyanobacteria blooms in
763 three eutrophic basins of the Great Lakes: a comparative analysis using satellite remote
764 sensing, Int. J. Remote Sens., 37, 4148–4171, https://doi.org/10.1080/01431161.2016.1207265,
765 2016.

766 Sayers, M. J., Bosse, K. R., Shuchman, R. A., Ruberg, S. A., Fahnenstiel, G. L., Leshkevich, G.
767 A., Stuart, D. G., Johengen, T. H., Burtner, A. M., and Palladino, D.: Spatial and temporal
768 variability of inherent and apparent optical properties in western Lake Erie: Implications for
769 water quality remote sensing, J. Gt. Lakes Res., 45, 490–507,
770 https://doi.org/10.1016/j.jglr.2019.03.011, 2019.

771 Smith, D. J., Tan, J. Y., Powers, M. A., Lin, X. N., Davis, T. W., and Dick, G. J.: Individual
772 Microcystis colonies harbour distinct bacterial communities that differ by Microcystis oligotype
773 and with time, Environ. Microbiol., 23, 3020–3036, https://doi.org/10.1111/1462-2920.15514,
774 2021.

775 Smith, D. J., Berry, M. A., Cory, R. M., Johengen, T. H., Kling, G. W., Davis, T. W., and Dick, G.
776 J.: Heterotrophic Bacteria Dominate Catalase Expression during Microcystis Blooms, Appl.
777 Environ. Microbiol., 88, e02544-21, https://doi.org/10.1128/aem.02544-21, 2022.

778    Smith, R. B., Bass, B., Sawyer, D., Depew, D., and Watson, S. B.: Estimating the economic
779    costs of algal blooms in the Canadian Lake Erie Basin, Harmful Algae, 87, 101624,
780    https://doi.org/10.1016/j.hal.2019.101624, 2019.

781    Speziale, B. J., Schreiner, S. P., Giammatteo, P. A., and Schindler, J. E.: Comparison of N,N-
782    Dimethylformamide, Dimethyl Sulfoxide, and Acetone for Extraction of Phytoplankton
783    Chlorophyll, Can. J. Fish. Aquat. Sci., 41, 1519–1522, https://doi.org/10.1139/f84-187, 1984.

784    Standard Methods Committee of the American Public Health Association, American Water
785    Works Association, and Water Environment Federation: Standard Methods For the Examination
786    of Water and Wastewater, 23$^{rd}$ edition, Sections 2540 Solids, 4500-P Phosphorus, 4500-nh3-
787    nitrogen (ammonia), 4500-no3-nitrogen (nitrate), 5310 Total Organic Carbon, edited by: Lipps
788    WC, Baxter TE, Braun-Howland E, APHA Press, Washington, DC, ISBN 1625762402, 2017.

789    Steffen, M. M., Belisle, B. S., Watson, S. B., Boyer, G. L., and Wilhelm, S. W.: Status, causes
790    and controls of cyanobacterial blooms in Lake Erie, J. Gt. Lakes Res., 40, 215–225,
791    https://doi.org/10.1016/j.jglr.2013.12.012, 2014.

792    Steffen, M. M., Davis, T. W., McKay, R. M. L., Bullerjahn, G. S., Krausfeldt, L. E., Stough, J. M.
793    A., Neitzey, M. L., Gilbert, N. E., Boyer, G. L., Johengen, T. H., Gossiaux, D. C., Burtner, A. M.,
794    Palladino, D., Rowe, M. D., Dick, G. J., Meyer, K. A., Levy, S., Boone, B. E., Stumpf, R. P.,
795    Wynne, T. T., Zimba, P. V., Gutierrez, D., and Wilhelm, S. W.: Ecophysiological Examination of
796    the Lake Erie Microcystis Bloom in 2014: Linkages between Biology and the Water Supply
797    Shutdown of Toledo, OH, Environ. Sci. Technol., 51, 6745–6755,
798    https://doi.org/10.1021/acs.est.7b00856, 2017.

799    Sterner, R. W., Keeler, B., Polasky, S., Poudel, R., Rhude, K., and Rogers, M.: Ecosystem
800    services of Earth's largest freshwater lakes, Ecosyst. Serv., 41, 101046,
801    https://doi.org/10.1016/j.ecoser.2019.101046, 2020.

802    Stow, C. A., Cha, Y., Johnson, L. T., Confesor, R., and Richards, R. P.: Long-Term and
803    Seasonal Trend Decomposition of Maumee River Nutrient Inputs to Western Lake Erie, Environ.
804    Sci. Technol., 49, 3392–3400, https://doi.org/10.1021/es5062648, 2015.

805    Stumpf, R. P., Davis, T. W., Wynne, T. T., Graham, J. L., Loftin, K. A., Johengen, T. H.,
806    Gossiaux, D., Palladino, D., and Burtner, A.: Challenges for mapping cyanotoxin patterns from
807    remote sensing of cyanobacteria, Harmful Algae, 54, 160–173,
808    https://doi.org/10.1016/j.hal.2016.01.005, 2016.

809    US EPA - United States Environmental Protection Agency: Method 180.1: Determination of
810    Turbidity by Nephelometry, Revision 2.0, Edited by: O'Dell, J.W., 1993.

811    US EPA - United States Environmental Protection Agency: Drinking Water Health Advisory for
812    the Cyanobacterial Microcystin Toxins, EPA Document Number 820R15100, 2015.
813
814    Van Meter, K. J., McLeod, M. M., Liu, J., Tenkouano, G. T., Hall, R. I., Van Cappellen, P., and
815    Basu, N. B.: Beyond the Mass Balance: Watershed Phosphorus Legacies and the Evolution of
816    the Current Water Quality Policy Challenge, Water Resour. Res., 57, e2020WR029316,
817    https://doi.org/10.1029/2020WR029316, 2021.

818    Vander Woude, A., Ruberg, S., Johengen, T., Miller, R., and Stuart, D.: Spatial and temporal
819    scales of variability of cyanobacteria harmful algal blooms from NOAA GLERL airborne
820    hyperspectral imagery, J. Gt. Lakes Res., 45, 536–546,
821    https://doi.org/10.1016/j.jglr.2019.02.006, 2019.

822    Vanderploeg, H. A., Liebig, J. R., Carmichael, W. W., Agy, M. A., Johengen, T. H., Fahnenstiel,
823    G. L., and Nalepa, T. F.: Zebra mussel (Dreissena polymorpha) selective filtration promoted
824    toxic Microcystis blooms in Saginaw Bay (Lake Huron) and Lake Erie, Can. J. Fish. Aquat. Sci.,
825    58, 1208–1221, https://doi.org/10.1139/f01-066, 2001.

826    Wang, Q. and Boegman, L.: Multi-Year Simulation of Western Lake Erie Hydrodynamics and
827    Biogeochemistry to Evaluate Nutrient Management Scenarios, Sustainability, 13, 7516,
828    https://doi.org/10.3390/su13147516, 2021.

829    Watson, S. B., Miller, C., Arhonditsis, G., Boyer, G. L., Carmichael, W., Charlton, M. N.,
830    Confesor, R., Depew, D. C., Höök, T. O., Ludsin, S. A., Matisoff, G., McElmurry, S. P., Murray,
831    M. W., Peter Richards, R., Rao, Y. R., Steffen, M. M., and Wilhelm, S. W.: The re-eutrophication
832    of Lake Erie: Harmful algal blooms and hypoxia, Harmful Algae, 56, 44–66,
833    https://doi.org/10.1016/j.hal.2016.04.010, 2016.

834    Weiskerger, C. J., Rowe, M. D., Stow, C. A., Stuart, D., and Johengen, T.: Application of the
835    Beer–Lambert Model to Attenuation of Photosynthetically Active Radiation in a Shallow,
836    Eutrophic Lake, Water Resour. Res., 54, 8952–8962, https://doi.org/10.1029/2018WR023024,
837    2018.

838    Wetzel, R.G., and Likens G.E.: Limnological Analyses, 3$^{rd}$ edition, Springer New York, NY,
839    https://doi.org/10.1007/978-1-4757-3250-4, 2000.

840    WHO - World Health Organization: Cyanobacterial toxins: microcystins. Background document
841    for development of WHO Guidelines for drinking-water quality and Guidelines for safe
842    recreational water environments, WHO/HEP/ECH/WSH/2020.6, 2020.
843

844    Wilson, A. E., Gossiaux, D. C., Höök, T. O., Berry, J. P., Landrum, P. F., Dyble, J., and
845    Guildford, S. J.: Evaluation of the human health threat associated with the hepatotoxin
846    microcystin in the muscle and liver tissues of yellow perch (Perca flavescens), Can. J. Fish.
847    Aquat. Sci., 65, 1487–1497, https://doi.org/10.1139/F08-067, 2008.

848    Wynne, T. T., Stumpf, R. P., Tomlinson, M. C., Fahnenstiel, G. L., Dyble, J., Schwab, D. J., and
849    Joshi, S. J.: Evolution of a cyanobacterial bloom forecast system in western Lake Erie:
850    Development and initial evaluation, J. Gt. Lakes Res., 39, 90–99,
851    https://doi.org/10.1016/j.jglr.2012.10.003, 2013.

852    Xu, J., Liu, H., Lin, J., Lyu, H., Dong, X., Li, Y., Guo, H., and Wang, H.: Long-term monitoring
853    particulate composition change in the Great Lakes using MODIS data, Water Res., 222,
854    118932, https://doi.org/10.1016/j.watres.2022.118932, 2022.

855    Yancey, C.E., Mathiesen, O., and Dick, G.J.: Transcriptionally active nitrogen fixation and
856    biosynthesis of diverse secondary metabolites by Dolichospermum and Aphanizominom-like
857    Cyanobacteria in western Lake Erie Microcystis blooms, bioRxiv [preprint],
858    https://doi.org/10.1101/2022.09.30.510322  01 October 2022a.

859     Yancey, C. E., Smith, D. J., Den Uyl, P. A., Mohamed, O. G., Yu, F., Ruberg, S. A., Chaffin, J.
860     D., Goodwin, K. D., Tripathi, A., Sherman, D. H., and Dick, G. J.: Metagenomic and
861     Metatranscriptomic Insights into Population Diversity of Microcystis Blooms: Spatial and
862     Temporal Dynamics of mcy Genotypes, Including a Partial Operon That Can Be Abundant and
863     Expressed, Appl. Environ. Microbiol., 88, e02464-21, https://doi.org/10.1128/aem.02464-21,
864     2022b.